Trastuzumab cotreatment improves survival of mice with PC-3 prostate cancer xenografts treated with the GRPR antagonist ^{177}Lu-DOTAGA-PEG$_2$-RM26

Bogdan Mitran[1], Sara S. Rinne[1], Mark W. Konijnenberg[2], Theodosia Maina[3], Berthold A. Nock[3], Mohamed Altai[4], Anzhelika Vorobyeva[4], Mats Larhed[1,5], Vladimir Tolmachev[4], Marion de Jong[2], Ulrika Rosenström[1] and Anna Orlova [ORCID][1,5]

[1]Department of Medicinal Chemistry, Uppsala University, Uppsala, Sweden
[2]Department of Radiology & Nuclear Medicine, Erasmus MC, Rotterdam, The Netherlands
[3]Molecular Radiopharmacy, INRASTES, NCSR "Demokritos", Athens, Greece
[4]Department of Immunology, Genetics and Pathology, Uppsala University, Uppsala, Sweden
[5]Science for Life Laboratory, Uppsala University, Uppsala, Sweden

Gastrin-releasing peptide receptors (GRPRs) are overexpressed in prostate cancer and are suitable for targeted radionuclide therapy (TRT). We optimized the bombesin-derived GRPR-antagonist PEG$_2$-RM26 for labeling with ^{177}Lu and further determined the effect of treatment with ^{177}Lu-labeled peptide alone or in combination with the anti-HER2 antibody trastuzumab in a murine model. The PEG$_2$-RM26 analog was coupled to NOTA, NODAGA, DOTA and DOTAGA chelators. The peptide-chelator conjugates were labeled with ^{177}Lu and characterized *in vitro* and *in vivo*. A preclinical therapeutic study was performed in PC-3 xenografted mice. Mice were treated with intravenous injections (6 cycles) of (A) PBS, (B) DOTAGA-PEG$_2$-RM26, (C) ^{177}Lu-DOTAGA-PEG$_2$-RM26, (D) trastuzumab or (E) ^{177}Lu-DOTAGA-PEG$_2$-RM26 in combination with trastuzumab. ^{177}Lu-DOTAGA-PEG$_2$-RM26 demonstrated quantitative labeling yield at high molar activity (450 GBq/μmol), high *in vivo* stability (5 min pi >98% of radioligand remained when coinjected with phosphoramidon), high affinity to GRPR ($K_D = 0.4 \pm 0.2$ nM), and favorable biodistribution (1 hr pi tumor uptake was higher than in healthy tissues, including the kidneys). Therapy with ^{177}Lu-DOTAGA-PEG$_2$-RM26 induced a significant inhibition of tumor growth. The median survival for control groups was significantly shorter than for treated groups (Group C 66 days, Group E 74 days). Trastuzumab together with radionuclide therapy significantly improved survival. No treatment-related toxicity was observed. In conclusion, based on *in vitro* and *in vivo* characterization of the four ^{177}Lu-labeled PEG$_2$-RM26 analogs, we concluded that ^{177}Lu-DOTAGA-PEG$_2$-RM26 was the most promising analog for TRT. Radiotherapy using ^{177}Lu-DOTAGA-PEG$_2$-RM26 effectively inhibited tumor growth *in vivo* in a murine prostate cancer model. Anti-HER2 therapy additionally improved survival.

Cancer Therapy and Prevention

What's new?

Targeted radionuclide therapy (TRT) using radiolabeled peptides seeking gastrin-releasing peptide receptors (GRPRs) in tumors is a promising approach to treat disseminated prostate cancer. The possibility to improve the therapeutic index *via* combination therapies also warrants further investigation. Here, the authors developed and characterized a promising GRPR-targeting radioligand and demonstrated its therapeutic efficacy in prostate cancer xenografts. Moreover, this study using the anti-HER2 antibody trastuzumab presents the first *in vivo* proof-of-principle that the effects of anti-GRPR radiotherapy can be amplified by co-administration of anti-HER2 treatment leading to prolonged survival.

Introduction

Prostate cancer is the most frequently diagnosed cancer and the second leading cause of cancer-related death in men. Similar to other cancers, over 90% of prostate cancer-related deaths are due to widespread metastatic disease. With the recent advancements in molecular imaging, metastatic prostate cancer patients can be classified into different prognostic subgroups depending on the metastatic spread, such as oligometastatic, polymetastatic or oligorecurrent cancers.[1] These subgroups have a different progression course and can benefit from improved personalized treatment strategies directed against specific features of the pathology.

A promising therapeutic approach is the use of radiolabeled probes for targeted radionuclide therapy (TRT). TRT is based on the use of high-affinity radiolabeled molecules designed to bind to molecular targets on the surface of tumor cells. This allows the selective delivery of systemically administered radioactivity to cancer cells while limiting radiation exposure to healthy tissues. An additional advantage of TRT, especially in the context of the highly heterogeneous nature of prostate cancer, is the ability to hit tumor cells that do not express the targeted receptor via the crossfire effect.

Peptides are attractive vehicles for TRT because of their rapid clearance, fast tumor penetration, low immunogenicity, inexpensive production and well-established bioconjugation and radiolabeling strategies. The successful introduction of somatostatin analogs for peptide receptor-mediated TRT in neuroendocrine tumors[2] paved the way for other radiopeptides targeting G-protein-coupled receptors, such as bombesin analogs targeting gastrin-releasing peptide receptors (GRPRs) overexpressed on tumor cells.

GRPRs have been found to be overexpressed in primary prostate cancer (63–100%), lymph node metastases (86%) and bone metastases (53%) but not in the hyperplastic prostate.[3,4] Importantly, GRPRs are highly expressed in the early stages of prostate cancer, therefore emerging as attractive targets for therapies directed against the oligometastatic state of prostate cancer—a transient step in the metastatic process between localized disease and widespread metastases. Bombesin is an amphibian linear tetradecapeptide with a high affinity for the human GRPRs. Several derivatives of bombesin have been developed over the past decades for diagnostic and/or therapeutic purposes. The field was initially focused on bombesin agonists due to the rapid radioligand internalization.[5] However, the superior results reported for somatostatin antagonists[6] led to a change of paradigm in the development of bombesin analogs toward potent GRPR-antagonists.[7]

We have recently investigated several constructs based on the GRPR-antagonist RM26 [(D-Phe^6,Sta^{13},Leu^{14}-NH$_2$) bombesin(6–14)].[8,9] It is known that pharmacokinetics and targeting properties of small peptides and proteins may be altered by structural modifications.[10] Therefore, we investigated the influence of different length of PEG linkers (n = 2, 3, 4, 6) and different chelating moieties (NOTA, NODAGA, DOTA, DOTAGA) on the *in vivo* imaging properties of resulting radioligands. The effects of the PEG spacer's length on overall hydrophilicity were found to be minor.[11] However, the use of different macrocyclic chelators had a profound influence on the biodistribution profile of the radiolabeled conjugates.[12,13] In this regard, both the geometry and the net charge of the radionuclide–chelator complex were identified as important factors influencing the blood clearance, activity uptake in tumors and normal organs, and kidney activity retention.

The optimal chelator–radionuclide pair resulted in exceptionally high tumor-to-organ ratios suggesting that X-PEG$_2$-RM26 could be exploited for TRT against GRPR using a therapeutic radiometal such as lutetium-177. Lutetium-177 is a β$^-$-emitter with half-life of 6.71 days and maximum energy of 0.5 MeV, resulting in a maximal tissue penetration of <2 mm, most suitable for irradiation of small lesions. The accompanying gamma photons (113 keV, 6.4% and 208 keV, 11%) of ^{177}Lu allow for single photon emission computed tomography (SPECT) acquisition, favoring the application of this attractive radioisotope in a theranostic setting.[14] A systematic search for the most suitable chelator for coupling to the biomolecule of interest, namely PEG$_2$-RM26, is expected to help optimize the final radioligand profile.

In addition to the great potential of GRPR-targeting radiotherapy approaches, the opportunity to further improve therapeutic index *via* combination therapies should be investigated. These combination therapies often consist of simultaneous application of different mechanisms of action and have been increasingly implemented in the clinic in the past years, showing superior results over monotherapies. Initially, prostate cancer is hormone-dependent and hence androgen deprivation therapy (ADT) generally leads to transient remissions. However, patients will eventually develop resistance to ADT and experience disease progression towards castration-resistant prostate cancer (CRPC) which is highly resistant to cytotoxic drugs and is invariably fatal.[15,16] Progression of CRPC is often driven by growth factors and their receptors, and abnormal levels of growth factors have been observed in tissue specimens collected from prostate cancer patients.[17] The epidermal growth factor

Cancer Therapy and Prevention

receptors (EGFR) family plays important roles in regulating cell proliferation, survival and differentiation, acting through ErbB or HER receptors including EGFR (HER1 or ErB-1), HER2/neu (ErbB-2), HER3 (ErbB-3) and HER4 (ErbB-4). Likewise, abnormal expression and activity of some of these receptors have been reported in prostate cancer. Most notably, HER-2/neu was shown to be overexpressed and to have an important role in the development of castration-resistant disease.[18,19]

In a recent study, Andersson *et al.* showed that HER-2/neu expression in androgen-independent PC-3 prostate cancer cells significantly increased after external irradiation leading to resistance to therapy.[20] The subsequent postirradiation treatment with the anti-HER-2/neu monoclonal antibody trastuzumab resulted in a twofold decrease in the PC-3 cell survival *in vitro*. Therefore, we hypothesized that the inhibition of this prosurvival signaling pathway could amplify tumor response to TRT.

The aim of our study was to determine the factors influencing the effects of treatment with the ^{177}Lu-labeled GRPR-antagonist PEG$_2$-RM26 in a murine model. To reach this goal, we first investigated the influence of chelators on the labeling, stability, binding affinity and biodistribution profile of ^{177}Lu-labeled PEG$_2$-RM26 and identified the most suitable construct for the subsequent GRPR-TRT. *In vivo* degradation of radiopeptides by proteolytic enzymes can limit their successful application as theranostic probes. Therefore, in our study, we have also evaluated the influence of the neprilysin (NEP) inhibitor phosphoramidon (PA) on the stabilization of radiopeptides *in vivo*. Finally, we explored if HER-2/neu could be targeted concomitantly with GRPRs in our model thereby improving therapeutic outcome.

Materials and Methods

Detailed descriptions of materials, equipment and methods used in our study are given in the Supporting Information

The synthesis of X-PEG$_2$-RM26 (X = NOTA, NODAGA, DOTA, DOTAGA) by solid-phase peptide synthesis (SPPS) was previously reported[12] (Supporting Information Fig. S1). No carrier added ^{177}LuCl$_3$ was purchased from Curium Pharma and ITG Isotopes Technologies Garching GmbH. *In vitro* cell studies were performed using PC-3 human prostate adenocarcinoma cells expressing the GRPR (ATCC, LGC Promochem).

Data were analyzed by an unpaired, two-tailed *t*-test or one-way ANOVA with Bonferroni correction for multiple comparisons using GraphPad Prism (version 7.03 for Windows GraphPad Software, La Jolla, CA) to determine significant statistical differences ($p < 0.05$).

Labelings of X-PEG$_2$-RM26 for *in vitro* and *in vivo* evaluation is described in details in the Supporting Information. High molar activity labeling studies (≈300 MBq/nmol) were performed using 1.3 nmol of DOTAGA-PEG$_2$-RM26 in 40 μl of 1 M ascorbic acid pH 5.5, followed by incubation with ^{177}Lu-chloride at 85°C for 30 min. The activity concentration of ^{177}Lu solution used for labeling was ≈400 MBq/30 μl. The

radiochemical yield was determined by instant thin-layer chromatography (ITLC) and high-performance liquid chromatography (HPLC). Labeling stability was evaluated in murine serum.

In vitro binding specificity, cellular processing and kinetics of binding to and dissociation from living cells were evaluated using PC-3 cells as previously described.[13]

Animal experiments were planned and performed in accordance with the national legislation on the protection of laboratory animals, and the study plans were approved by the local committee for animal research ethics. BALB/c nu/nu mice bearing PC-3 xenografts were used for *in vivo* studies.

The *in vivo* metabolic stability of radioligands without or with coinjection of PA was evaluated in healthy male Swiss albino mice (30 ± 5 g, NCSR "Demokritos" Animal House Facility) 5 min pi of ^{177}Lu-X-PEG$_2$-RM26 (X = NODAGA, DOTA, DOTAGA) based on previously reported methods.[21]

For comparative biodistribution studies, mice were injected with 50 pmol (120 kBq, 100 μl) of ^{177}Lu-X-PEG$_2$-RM26 (X = NODAGA, DOTA, DOTAGA) and euthanized at 1 and 24 hr pi. The influence of coinjection of PA on the biodistribution of ^{177}Lu-DOTAGA-PEG$_2$-RM26 (88 kBq, 100 μl) at 50 pmol total peptide dose was studied at 1 hr pi. To investigate the influence of injected peptide dose on tumor targeting and biodistribution profile at 1 hr pi of ^{177}Lu-DOTAGA-PEG$_2$-RM26, the administrated peptide dose was adjusted to 50, 100, 250, 500 and 750 pmol. Biodistribution of ^{177}Lu-DOTAGA-PEG$_2$-RM26 (80 kBq, 100 μl) overtime at the 100 pmol peptide dose was studied in the time interval between 30 min and 92 hr pi. Activity distribution on tumor sections was evaluated using receptor autoradiography. *In vitro* and *in vivo* HER2 expression in PC-3 cells was confirmed using ^{68}Ga-labeled ABY-025, a second-generation affibody scaffold protein with a high affinity to HER2 receptor.[22]

Estimation of the organs' absorbed doses was done for the injection of 100 pmol of ^{177}Lu-DOTAGA-PEG$_2$-RM26, using the biodistribution data over time and a MOBY-phantom based dosimetry model.[23] Dosimetry estimates were made for other peptide masses by using the ratios in the 1 hr uptake values at 50–250 pmol with the 100 pmol 1 hr uptake data (Supporting Information Fig. S2). Tumor control probability was compared for tumors of 200 and 100 mm^3 for protocols including six therapy cycles within 2 weeks, using the PC-3 radiation sensitivity parameters, derived from Carlson *et al.*[24]

Experimental *in vivo* therapy

For *in vivo* therapy, five experimental groups (*n* = 11–12) were treated every second day for 2 weeks (6 cycles): Group A with PBS; Group B with DOTAGA-PEG$_2$-RM26 (200 pmol); Group C with ^{177}Lu-DOTAGA-PEG$_2$-RM26 (200 pmol/60 MBq); Group D with trastuzumab (5 mg/kg); Group E with ^{177}Lu-DOTAGA-PEG$_2$-RM26 (200 pmol/60 MBq) in combination with trastuzumab (5 mg/kg). Average tumor size was 105 ± 28 mm^3. Groups B, C and E were coinjected with PA (300 μg/mouse). Tumor uptake of activity was followed during treatment by single photon emission computed tomography/computed tomography (SPECT/CT) imaging on days

14, 16 and 25. One week after accomplished treatment, two animals/group were sacrificed; blood was collected for leukocyte counting and tumor, liver, kidneys and pancreas were taken for histological examination. The mice were monitored two times weekly. Mice were euthanized when they lost more than 15% of their original mass, when tumor ulceration occurred or when tumor volume exceeded 1 cm^3. At end point, tumors, kidneys, liver and pancreas were collected and histologically evaluated ($n = 3$, the longest survivals).

Results

Radiolabeling

Radiolabeling of X-PEG$_2$-RM26 with ^{177}Lu was achieved in high yields (Table 1). Because of the high radiolabeling yields obtained for NODAGA, DOTA and DOTAGA-containing analogs, these tracers were used without purification for further experiments. An *in vitro* serum stability test revealed very good serum stability for ^{177}Lu-DOTA-PEG$_2$-RM26 and ^{177}Lu-DOTAGA-PEG$_2$-RM26 with less than 1.5% free radiometal release after 1 hr incubation at 37°C. A higher activity release was observed for ^{177}Lu-NODAGA-PEG$_2$-RM26. The pronounced release of ^{177}Lu observed for ^{177}Lu-NOTA-PEG$_2$-RM26, indicated a poor radiometal–chelate complex stability for this analog.

For therapy, ^{177}Lu-DOTAGA-PEG$_2$-RM26 was successfully labeled with ^{177}Lu in a higher than 99.5% radiolabeling yield at a maximum molar activity of 450 MBq/nmol (Supporting Information Fig. S3).

In vitro studies

Binding of ^{177}Lu-X-PEG$_2$-RM26 to GRPR-expressing PC-3 cells was significantly reduced by presaturation of receptors with excess of nonlabeled peptide, indicating receptor-mediated binding (Supporting Information Fig. S4). The binding of all analogues was rapidly reaching approximately 70% of maximum cell-associated activity after 1 hr incubation (Supporting Information Fig. S5). The cell-associated radioactivity reached a plateau after 4 hr for all conjugates with the exception of ^{177}Lu-DOTAGA-PEG$_2$-RM26 where it gradually increased up to the 24 hr time-point. The internalization pattern was similar for all analogs showing a low fraction of

internalized radioactivity typical for GRPR-antagonists that could be explained by cell surface renewal. The measurements of binding kinetics of ^{177}Lu-X-PEG$_2$-RM26 in real time showed sub-nanomolar equilibrium dissociation constant (K_D) values for all analogs (Table 1).

The presence of HER-2/neu on PC-3 cells *in vitro* was confirmed by a binding specificity assay using ^{68}Ga-labeled anti-HER2 affibody ABY025 (Fig. 5a).

In vivo studies

In vivo *metabolic stability of* ^{177}*Lu-X-PEG$_2$-RM26 (X = NODAGA, DOTA, DOTAGA)*. Metabolic stability was tested for ^{177}Lu-X-PEG$_2$-RM26 (X = NODAGA, DOTA, DOTAGA) in Swiss albino mice (Table 1, Supporting Information Fig. S6). The NOTA-modified conjugate was excluded from *in vivo* characterization due to poor *in vitro* stability of the radiometal-chelate. The *in vivo* formation of radiometabolites was studied by HPLC analysis of mouse blood samples collected at 5 min after injection of test-radiopeptide alone or coinjected with PA (Supporting Information Fig. S6). Within this period, ^{177}Lu-DOTAGA-PEG$_2$-RM26 exhibited the highest *in vivo* stability. Upon coinjection of PA, the stability of all tested radiopeptides increased significantly.

Comparative biodistribution of ^{177}*Lu-X-PEG$_2$-RM26 (X = NODAGA, DOTA, DOTAGA) in PC-3 tumor-bearing mice.* A comparative biodistribution study was performed in PC-3 xenografted mice at 1 and 24 hr pi to determine which of the radiolabeled conjugates is the most suitable for therapy (Figs. 1a and 1b, Supporting Information Table S1). Lumbar lymph nodes metastases were detected in this batch of animals and were collected from all mice. All analogs demonstrated rapid blood clearance. The body clearance was predominantly renal with low kidney retention for all tested radiopeptides at 1 hr pi. Radioactivity uptake in tumors and metastases exceeded uptake in all normal organs including excretory organs for all variants with the exception of pancreatic uptake for the NODAGA-modified analog. Activity uptake in tumors was significantly higher for DOTA and DOTAGA-carrying radioligands than for the NODAGA one. The activity uptake in tumors decreased by twofold at 24 hr pi. However, clearance of activity from blood and normal organs was faster

Table 1. Labeling yield (molar activity 3 MBq/nmol), metal-chelate stability in serum, GRPR binding affinity and *in vivo* metabolic stability of ^{177}Lu-X-PEG$_2$-RM26 (X = NOTA, NODAGA, DOTA and DOTAGA); *in vivo* metabolic stability determined in peripheral mouse blood collected at 5 min pi of test radioligand without or with coinjection of PA

	NOTA	NODAGA	DOTA	DOTAGA
Labeling yield, %	96 ± 3 (19)	99.4 ± 0.6 (24)	99.9 ± 0.2 (24)	99.8 ± 0.3 (28)
^{177}Lu-release, 37°C 1 hr in plasma	16 ± 2% (3)	4.3 ± 0.7% (3)	1.5 ± 0.2% (3)	1.6 ± 0.5% (3)
GRPR-binding affinity, K_D, pM	331 ± 95 (3)	225 ± 50 (3)	211 ± 88 (3)	431 ± 240 (3)
Intact radiopeptide, 5 min pi	n.a.	64 ± 2% (3)	65 ± 5% (3)	71 ± 3% (3)
Intact radiopeptide, 5 min pi (+ phosphoramidon)	n.a.	›96%[1] (2)	›96.5%[1] (2)	›98%[1] (2)

Data are presented as average ± standard deviation.
Values in parentheses represent the number of experiments.
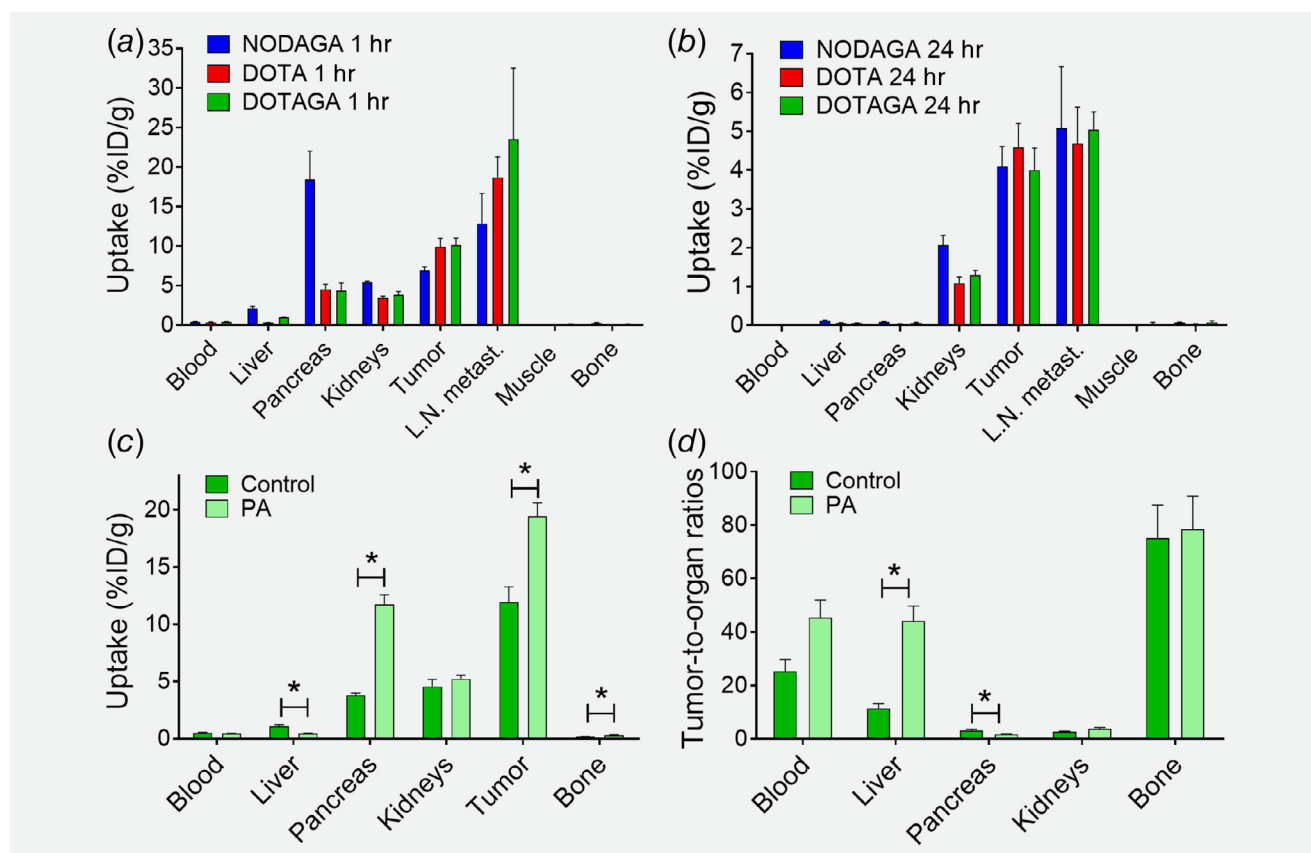[1]Values are not significantly different.

Figure 1. (*a, b*) Biodistribution of ^{177}Lu-X-PEG$_2$-RM26 (X = NODAGA, DOTA and DOTAGA) in PC-3 xenografted BALB/C nu/nu mice at 1 and 24 hr pi, respectively (50 pmol, 88 kBq/animal; mouse weight 15 ± 1 g; tumor weight 0.7 ± 0.2 g. (*c*) Influence of coadministration of PA on the biodistribution of ^{177}Lu-DOTAGA-PEG$_2$-RM26 in PC-3 xenografted BALB/C nu/nu mice at 1 hr (mouse weight 16 ± 2 g; tumor weight 0.17 ± 0.05 g). (*d*) Tumor-to-normal-tissue ratios at 1 hr.

than from tumors (Fig. 1*b*, Supporting Information Tables S1 and S2). ^{177}Lu-NODAGA-PEG$_2$-RM26 had the least favorable biodistribution profile at 1 hr pi with the lowest uptake in tumor and metastases and the highest radioactivity accumulation in liver and GRPR-expressing organs. Additionally, renal uptake was higher for this analog.

Influence of the NEP-inhibitor PA on the biodistribution of ^{177}Lu-DOTAGA-PEG$_2$-RM26. A biodistribution study was performed in PC-3 xenografted mice to determine the influence of PA-coinjection on activity uptake in tumors and normal organs (Figs. 1*c* and 1*d*, Supporting Information Table S3). Treatment with PA had a prominent impact on the uptake of ^{177}Lu-DOTAGA-PEG$_2$-RM26 (50 pmol) in tumor and in GRPR-expressing pancreas at 1 hr pi, presumably as a result of increased stabilization in blood circulation. In this regard, the tumor uptake increased 1.6-fold while pancreatic uptake increased threefold, resulting in a decrease in tumor-to-pancreas ratio. Coinjection of PA had no effect on kidney uptake. Consequently, tumor-to-kidney ratios have increased 1.4-fold. Delivering a high radioactivity dose to the notoriously radioresistant solid tumors is highly important, therefore further *in vivo* evaluation and therapy were performed with PA coinjection.

Influence of injected peptide mass on the biodistribution of ^{177}Lu-DOTAGA-PEG$_2$-RM26. In order to identify the optimal injected peptide dose, a comparative biodistribution study was performed at 1 hr pi of ^{177}Lu-DOTAGA-PEG$_2$-RM26 in a total peptide range 50–750 pmol (Fig. 2, Supporting Information Table S4). A strong blocking effect could be observed in tumors and GRPR-expressing organs with increasing peptide dose. Tumor uptake decreased threefold for 750 pmol in comparison to 50 pmol. Uptake in kidney and non-GRPR expressing organs was not influenced by injected peptide dose. As a result, tumor-to-kidney ratios decreased twofold for 750 pmol compared to 50 pmol (Fig. 2*b*, Supporting Information Table S5). However, autoradiography results indicated that despite superior uptake, tumor penetration was insufficient for the 50 pmol injected dose with most of the radioactivity located in the rim of the tumor (Fig. 2*c*). Activity distribution in tumors was homogeneous after injection of 100–250 pmol.

Biodistribution of ^{177}Lu-DOTAGA-PEG$_2$-RM26 *over time.* Data on the biodistribution of ^{177}Lu-DOTAGA-PEG$_2$-RM26 (100 pmol) in the period 0.5–90 hr pi are presented in Figure 3 and Supporting Information Table S6. ^{177}Lu-DOTAGA-PEG$_2$-RM26 displayed a rapid clearance from blood and background tissues. Tumor uptake
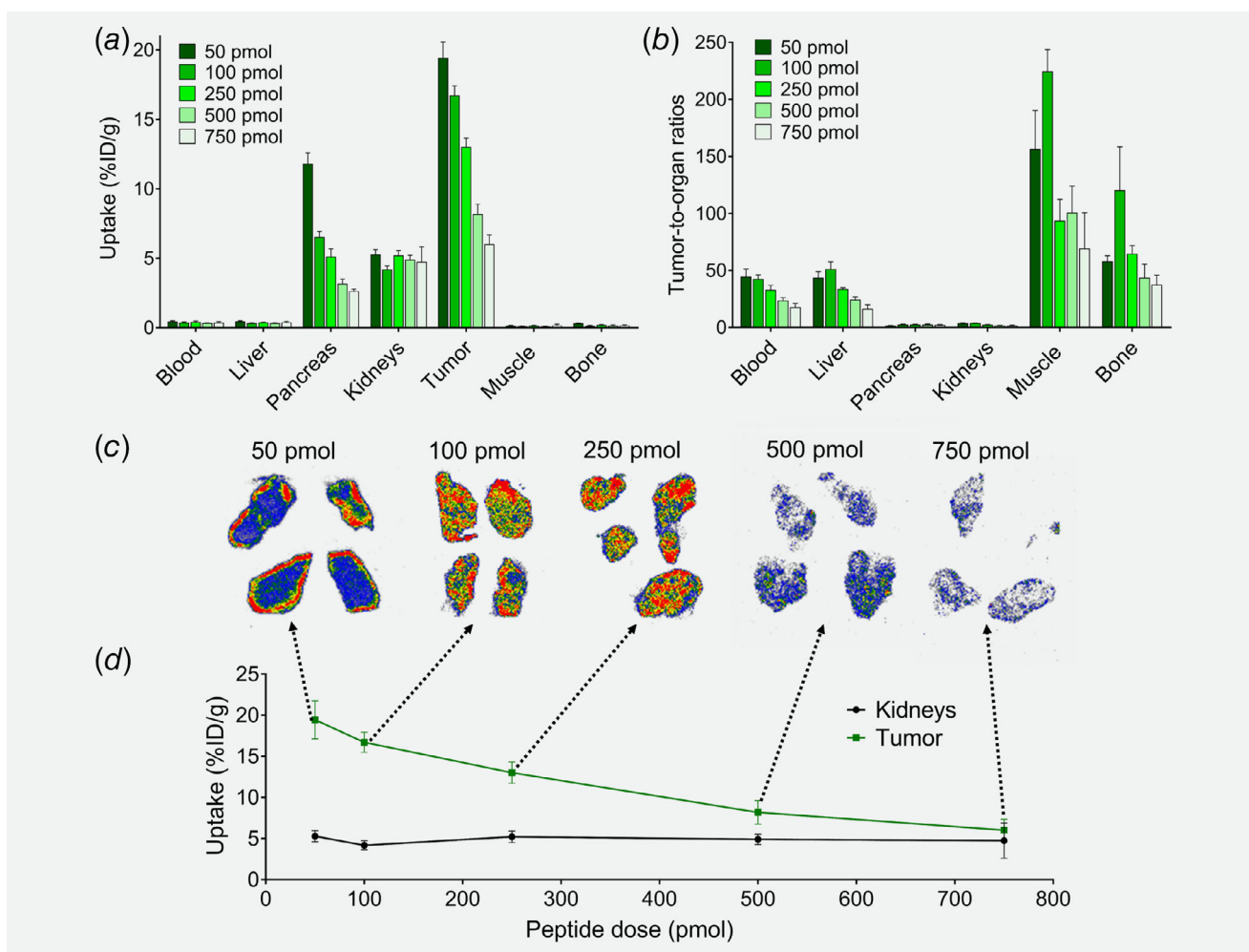
Figure 2. (*a*) Comparative biodistribution of different injected peptide doses (80 kBq in 50, 100, 250, 500 and 750 pmol/animal) of ^{177}Lu-DOTAGA-PEG$_2$-RM26 in BALB/C nu/nu mice bearing PC-3 tumors at 1 hr pi (mouse weight 17 ± 2 g; tumor weight 0.19 ± 0.06 g). (*b*) Tumor-to-normal-tissue ratios at 1 hr pi (50, 100, 250, 500 and 750 pmol/animal). (*c*) *Ex vivo* GRPR-autoradiography of tumor slices of mice bearing PC-3 tumors after the injection of ^{177}Lu-DOTAGA-PEG$_2$-RM26 (80 kBq in 50, 100, 250, 500 and 750 pmol) at 1 hr pi. (*d*) Uptake of activity in tumor and kidneys as a function of injected peptide dose.

peaked at 1 hr pi but decreased fourfold at 24 hr pi. The retention of radioactivity in the kidneys was low and a rapid decrease was observed within 24 hr pi. Tumor-to-kidney ratios increased three-fold from 0.5 hr pi up to 4 hr pi (Fig. 3*b*, Supporting Information Table S7). With time, due to the release of activity from tumors, tumor-to-kidney ratios decreased up to 90 hr pi. Nonetheless, tumor-to-kidney ratios were over 2 at all time-points. Autoradiography of tumor sections revealed a homogeneous uptake in tumors at all time-points and a slow washout of radioactivity from the tumor core (Fig. 3*c*).

Dosimetry. It was found that the protocol including six injections of 200 pmol/60 MBq of ^{177}Lu-DOTAGA-PEG$_2$-RM26 within 2 weeks should give good tumor control probability (Supporting Information Figs. 7A and S7B). Tumors with a size of 100 mm^3 should respond better to treatment compared to larger, 200 mm^3 tumors. The estimated absorbed doses per

60 MBq treatment cycle would be 11 Gy to the tumor, 5 Gy to the kidneys and 12 Gy to pancreas (Supporting Information Figs. S7C and S7D).

Therapy. The results of the *in vivo* therapy study are presented in Figure 4. Tumor growth was slower in both groups treated with radiolabeled peptide than in the control groups already after three therapy cycles (Fig. 4*a*). Tumor volumes were significantly smaller in treated groups compared to control group when therapy was accomplished ($p < 0.05$). However, there was no significant difference in tumor volumes between the groups treated with and without trastuzumab throughout the experiment. The majority of mice were sacrificed when tumors reached the maximum permitted volume or mice began to lose weight when tumor volume exceeded 0.75 cm^3, with few exceptions. Specifically, three mice had to be sacrificed due to critical weight loss (Groups A, C and D) and one due to tumor ulceration (Group D).
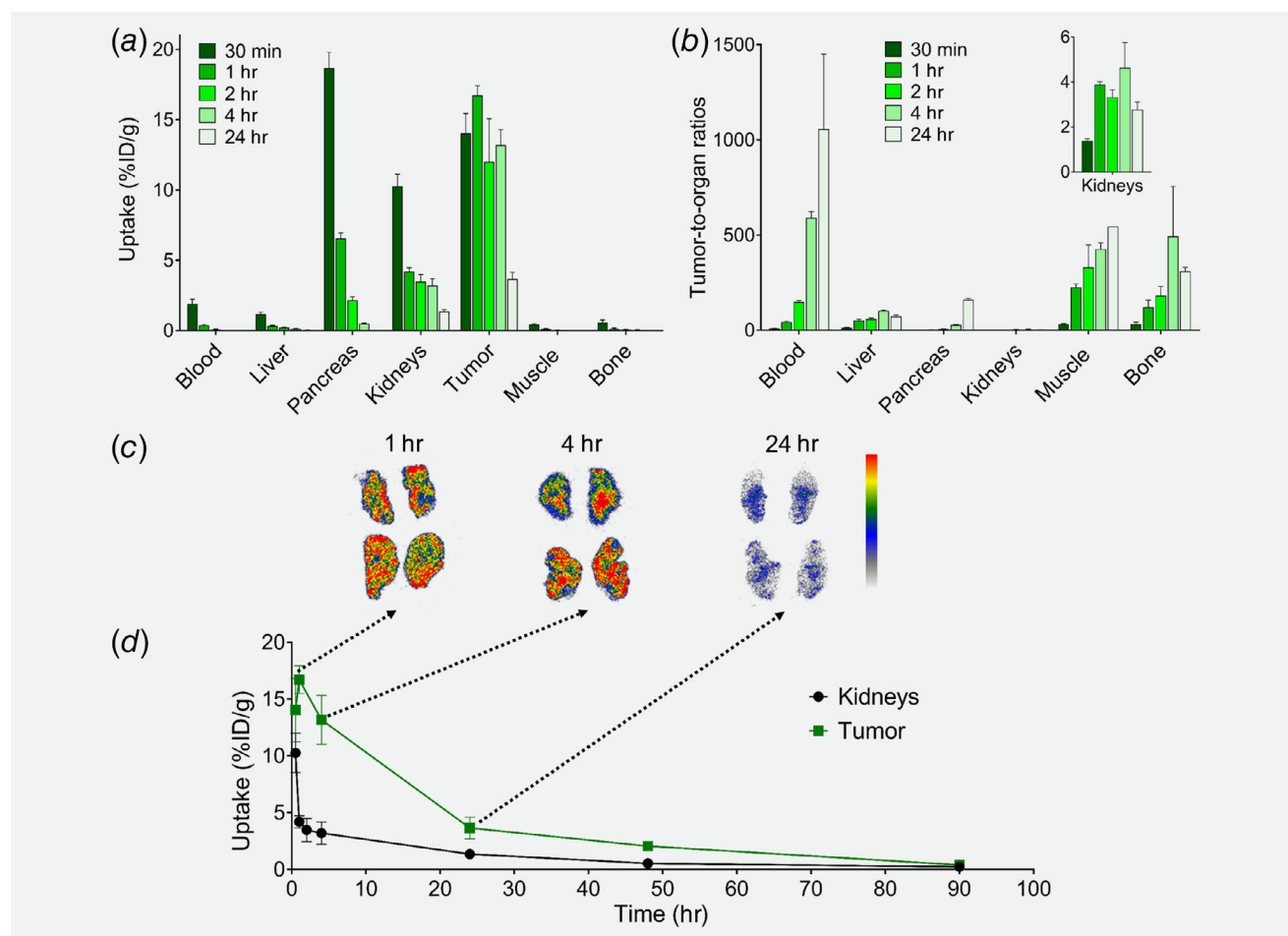
Figure 3. (*a*) Biodistribution of ^{177}Lu-DOTAGA-PEG$_2$-RM26 (80 kBq, 100 pmol/animal) over time (0.5, 1, 2, 4 and 24 hr pi) in PC-3-xenografted BALB/c nu/nu mice. (*b*) Tumor-to-normal-tissues ratios at 0.5, 1, 2, 4 and 24 hr pi (mouse weight 17 ± 2 g; tumor weight 0.2 ± 0.1 g). (*c*) *Ex vivo* GRPR-autoradiography of tumor slices of mice bearing PC-3 tumors after the injection of ^{177}Lu-DOTAGA-PEG$_2$-RM26 (100 pmol) at 1, 4 and 24 hr pi. (*d*) Uptake of activity in tumor and kidneys up to 90 hr pi.

Mice treated with unlabeled DOTAGA-PEG$_2$-RM26 or trastuzumab alone had the same median survival as the mice in vehicle group. Therapy with ^{177}Lu-DOTAGA-PEG$_2$-RM26 induced a significant prolongation of median survival for Group C compared to control Groups A, B and D ($p < 0.0001$). Coinjection of trastuzumab with radiolabeled peptide further improved median survival significantly ($p < 0.05$ for Groups C *vs.* E; Fig. 4*b*).

SPECT/CT scans acquired on days 14, 16 and 25 (after first, second and sixth injections) revealed a high initial uptake of radioactivity in GRPR-expressing tumors, followed by a pronounced decrease by the end of treatment (Fig. 4*d*).

Treatment was well tolerated, no weight loss or other signs of acute toxicity were detected (Fig. 4*c*). Follow up observations also did not detect any sign of toxicity, with the exception of some decrease in body weight in Groups A, B and D close to the end of the experiment. One week after the last cycle of therapy, two mice in each group were examined on leukocyte counts. Measured counts were within a narrow range for all groups (1.5–2.4×10^9/l).

Histological examination of kidneys, liver and pancreas was performed for mice sacrificed 1 week after therapy (2 mice/group) and mice with the longest survival time (3 mice/group). The liver, kidneys and pancreas did not show lesions that could be attributed to toxicity, and there were no specific histological differences between these organs in the different groups of the experiment.

Histological examination of tumors confirmed their localization in the dermis directly under the epidermis. The neoplastic cells were generally large, growing in a solid pattern and displayed obvious features of high malignancy (high pleomorphism, pronounced anisokaryosis, nuclear atypia, megalokaryosis, highly lobulated nuclei or polykaryons and high anaplasia). Mitotic activity was high with frequent atypical mitotic figures. There were extensive areas of necrosis in tumors harvested at endpoint and half of the animals in all groups at this point had metastases in the abdomen at varying sites: the capsule of the pancreas, liver and kidney, and the hepatic hilus. Metastases were not found within the parenchyma of the organs. Neither
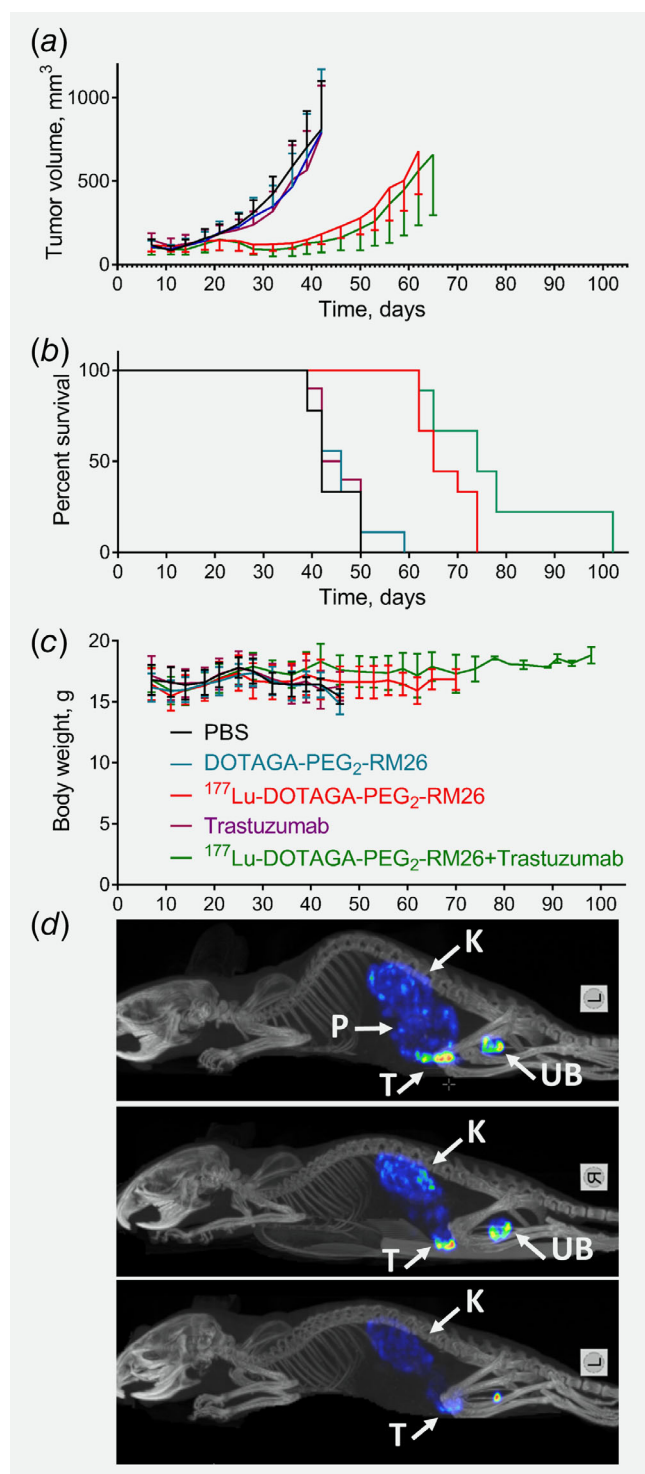
Cancer Therapy and Prevention

Figure 4. (*a, b, c*) The results of the *in vivo* therapy study in mice treated with: PBS (black line); nonlabeled peptide (DOTAGA-PEG₂-RM26, 200 pmol; teal line); ¹⁷⁷Lu-DOTAGA-PEG₂-RM26 (60 MBq/200 pmol; red line); trastuzumab (5 mg/kg; purple line); ¹⁷⁷Lu-DOTAGA-PEG₂-RM26 (60 MBq/200 pmol) in combination with trastuzumab (5 mg/kg; green line). (*d*) Representative SPECT/CT scans of ¹⁷⁷Lu-DOTAGA-PEG2-RM26 treated mice (red and green line). Mice were imaged 3 hr pi after first, second and six injections (from top). SPECT/CT images are presented as MIP in RGB color scale. Abbreviations: K, kidneys; UB, urinary bladder; T, tumor; P, pancreas.

tumors nor metastases had any pattern specific to the different treatments.

Immunohistochemical (IHC) examination of tumors in control group confirmed HER2 expression in PC-3 xenografts both at the start and the end of the experiment. These results were in agreement with PET imaging of HER2 expression using ⁶⁸Ga-ABY-025 (Fig. 5, Supporting Information Figs. S8 and S9). Weak membranous staining was detected in broad tumor areas in the control group. Similar pattern of HER2 expression was detected in the group treated with nonlabeled peptide. In the group treated with ¹⁷⁷Lu-labeled peptide, staining was more intensive after treatment but returned to weak with time (it should be noted that only limited tumor material was available in animals sacrificed after treatment; Fig. 5c). In the groups treated with trastuzumab at both time points, no HER2 expression was detected.

Discussion

Recent progress in the treatment of metastatic prostate cancer applying TRT (e.g. PSMA-targeting therapy using the beta-emitter lutetium-177 or the alpha-emitter actinium-225[24,25]) indicates that TRT might be utilized at earlier stages of prostate cancer. Success of TRT depends on many factors: the expression level of the molecular target in the lesion and healthy organs, the nature of the targeting molecule, its biodistribution pattern and excretion pathway, its pharmacokinetics and their matching to the physical properties of radioisotope employed as well as the size of targeted lesions. Taking into account the complexity of mechanisms driving cancer development and progression, it is reasonable to assume that TRT combined with therapies enhancing radiosensitivity should improve treatment outcome.[26]

Shifting of TRT toward oligometastatic prostate cancer might require reconsidering of the molecular target for therapy due to lower expression of PSMA at earlier stages of prostate cancer and its high expression in normal tissues (particularly in salivary and lacrimal glands and kidneys). Xerophthalmia and xerostomia are often side effects of TRT using PSMA inhibitors labeled with alpha- and beta-emitting radionuclides, which are the most suitable for oligometastatic disease.[25,27] The high expression levels of GRPR in the early stages of prostate cancer indicate that this receptor could be a promising supplementary molecular target for the treatment of oligometastatic prostate cancer.[3]

Short peptides based on natural ligands are attractive targeting agents for radiotherapy due to their rapid tissue penetration and rapid blood clearance. However, care should be taken (*i*) to achieve high *in vivo* stability to endogenous proteases, (*ii*) to avoid high renal reabsorption and (*iii*) to limit adverse effects elicited after binding and activation of the GRPR. Analogs of the GRPR-antagonist [D-Phe⁶,Sta¹³,Leu¹⁴-NH₂]bombesin(6–14) recently attracted attention as new molecular tools for TRT of prostate cancer. The above GRPR-antagonist was coupled with the DOTA chelator *via* different linkers and labeled with therapeutic radiometals, such as lutetium-177[2,28] or yttrium-90.[29] In all studies, a
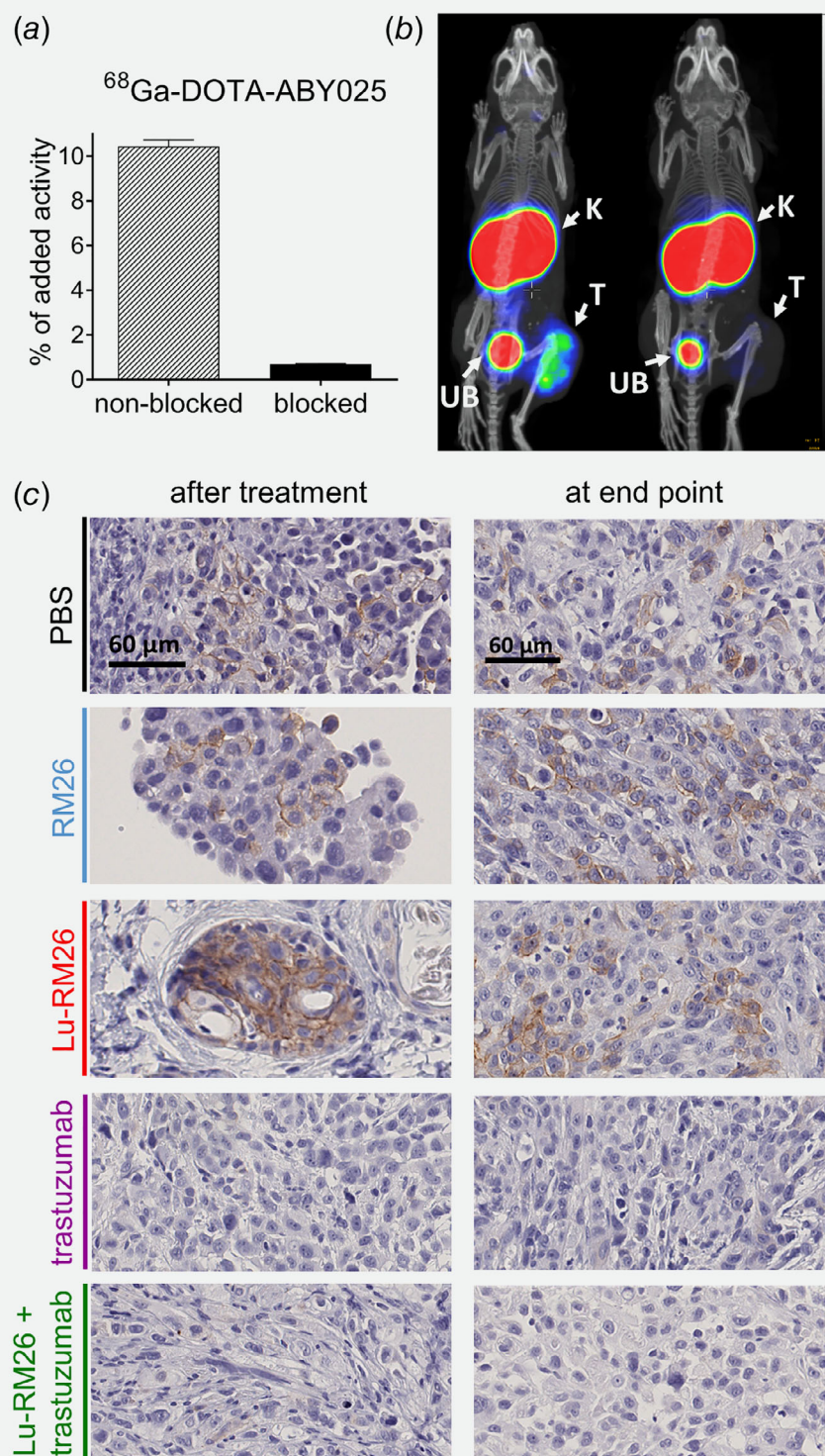
Figure 5. (*a*) *In vitro* binding specificity of anti-HER2 affibody molecule ^{68}Ga-ABY025 to PC-3 cells. Blocked cells were pretreated with a 100-fold excess of nonlabeled protein 10 min prior to the addition of 1 nM radiolabeled compound. Data are presented as the mean value of three dishes ± SD. (*b*) PET/CT imaging of HER2 expression in PC-3 xenografted mice at 2 hr pi. The mice were injected with 1 μg (0.2 MBq), left mouse, or a blocking dose (300 μg, 0.2 MBq), right mouse, of ^{68}Ga-labeled anti-HER2 affibody ABY025. PET/CT images are presented as MIP in RGB color scale. Abbreviations: K, kidneys; UB, urinary bladder; T, tumor. (*c*) Immunohistochemical staining of HER2 expression of 4 μm sections of paraffinated tissue samples of PC-3 xenografts. Samples were taken 1 week after therapy (left column) and at endpoint (right column).

Cancer Therapy and Prevention

significant delay of tumor growth was observed in animals treated with the radiopeptide. In the present work, we have modified the same GRPR-antagonist RM26 by coupling tri- and tetra-aza macrocyclic chelators to its N-terminus via a PEG$_2$-linker and investigated the respective ^{177}Lu-labeled radiopeptides for their efficacy in GRPR-targeted radiotherapy of prostate cancer in preclinical models. Previous studies have revealed a pronounced effect of the radiometal-chelate on the biodistribution of RM26 in mice.[12,13,30] Based on the newly acquired in vitro and in vivo data we have concluded that the tetra-aza chelators DOTAGA and DOTA resulted in ^{177}Lu-radioligands with the most suitable properties for TRT, showing a significantly higher tumor uptake compared to the NODAGA-carrying radioligand. This effect is most likely a result of the lower bioavailability of the NODAGA-containing analog due to its higher trapping in the pancreas and liver. ^{177}Lu-DOTAGA-PEG$_2$-RM26 had the best in vivo stability and was chosen for further evaluation.

In our further experiments, we focused on investigating the factors that would increase tumor-to-kidneys dose ratio. In general, renal toxicity is an important limitation for the applicability of radiotracers for TRT. The stabilization in peripheral blood by coinjection of the NEP-inhibitor PA with ^{177}Lu-DOTAGA-PEG$_2$-RM26 resulted in an impressive 60% amplification of tumor uptake at 1 hr pi, due to the higher supply of intact radioligand to the receptor-expressing tumor cells. As expected, the uptake in GRPR-expressing organs was also significantly increased, while the uptake in nontarget healthy tissues, particularly the kidneys were not affected. This strategy has been successfully used to enhance the efficacy of other peptide-based targeting vectors.[31–33]

An additional strategy for improving the ratio of tumor to kidney absorbed dose is to identify the optimal peptide mass. By gradually increasing the injected peptide dose, we observed a strong blocking effect on the tumor and the GRPR-expressing organs, but not in the kidneys and normal organs devoid of GRPR-expression. This observation contradicts with previously reported data for the similar GRPR antagonist RM2[28] and for GRPR agonists.[34] In both cases, tumor uptake was not influenced by peptide dose and remained stable up to 250–500 pmol. Interestingly, autoradiography of tumor samples provided a remarkable discovery: despite the highest tumor uptake, radioactivity distribution was concentrated primarily in the rim of tumors for the mice injected with 50 pmol. In contrast, tumor penetration was significantly better for the mice injected with 100 pmol and above. This phenomenon can be explained by the "Binding Site Barrier" model.[35] This model predicts that high-affinity binders at a given dose tend to have limited diffusion into tumors and by increasing the binder dose, a better percolation and more uniform distribution can be achieved. Efficient penetration into solid tumors is essential for improved therapeutic efficacy, especially when using ^{177}Lu that has a maximum penetration range in tissue of 2 mm.

Biodistribution results of ^{177}Lu-DOTAGA-PEG$_2$-RM26 (100 pmol) revealed a rapid clearance from blood, kidneys and normal nontarget organs. Tumor activity also cleared relatively fast within the first 24 hr pi. Nevertheless, tumor-to-kidney ratios were higher than 2 at all time-points. Simulations of injected peptide dose revealed that increase of injected peptide mass up to 200 pmol caused only 16% decrease in tumor-to-kidney ratios (Supporting Information Fig. S2B).

Based on this data, we designed a treatment protocol with multiple injections of radiopeptide to overcome the rapid wash-out of activity from tumors and performed an in vivo therapy study. In the present study, we demonstrated the potential of ^{177}Lu-DOTAGA-PEG$_2$-RM26 for targeted radiotherapy of prostate cancer. Tumor growth was significantly delayed in the groups treated with ^{177}Lu-DOTAGA-PEG$_2$-RM26. A decrease in tumor volume was observed already after three therapy cycles in the groups treated with radiolabeled peptide. Due to the inhibition of tumor growth, median survival was also significantly longer in these groups. Importantly, the increased survival was not associated with any detected side effects.

The most interesting finding of our study was the significant improvement of overall survival in the group treated with radiolabeled peptide plus trastuzumab. The HER2 protein is a notorious proto-oncogene that was shown to be implicated in a number of different cancers. In contrast to other cancers, HER2 is not considered a major driver of prostate cancer progression. The expression level of this receptor is generally low in prostate cancer. In the PC-3 tumor model used in our study, HER2-expression (~25,000 receptors/cell[36]) could be clinically considered as 1+ and HER2-targeted therapy alone is unlikely to inhibit tumor growth. Nonetheless, HER2 may have an important role as a resistance mechanism to other therapies. HER2 was found to be activated in prostate cancer after hormone therapy and patients suffering from metastatic prostate cancer were generally found to have higher levels of serum HER2 compared to those with early nonmetastatic disease.[37] In a recent in vitro study, Andersson et al. showed that HER2 expression in PC-3 cells increased significantly after external irradiation leading to resistance to therapy.[20]

Trastuzumab (Herceptin®) is an anti-HER2 antibody which has complex cytostatic action and is used for the treatment of HER2-positive breast cancers.[38] Trastuzumab alone does not give any therapeutic benefits to HER2-negative patients or patients with low HER2 expression. To increase treatment output, trastuzumab therapy is often combined with nonanthracycline-based chemotherapy and endocrine therapy. More recently trastuzumab–emtansine, an antibody–drug conjugate that combines the antitumor properties of trastuzumab with the cytotoxic effects of a microtubule-disrupting chemotherapy drug mertansine, was introduced.

In our study, the coinjection of trastuzumab together with the radiolabeled peptide significantly improved the overall survival. In agreement with clinical data, antiHER2 treatment did not induce any measurable therapeutic effect, however,

IHC HER2 staining demonstrated that even short treatment with trastuzumab eliminated HER2 expression. Interestingly, in agreement with our *in vitro* data,[20] HER2 expression increased shortly after radiotherapy in the group treated with the radiopeptide but was not detected in the group treated with the combination of radiopeptide and trastuzumab. The absence of HER2 expression shortly after therapy could be attributed to continued saturation of HER2 with trastuzumab. However, the absence of HER2 expression was confirmed in these groups at the endpoint.

Taking into account that trastuzumab has a complex mechanism of action on HER2-expressing cells, it is difficult to pinpoint the particular mechanism that is involved in this radiosensitizing effect. We could speculate that blocking of HER2 with trastuzumab decreased the repairing ability of irradiated cells. This finding is in agreement with a recent study demonstrating that the effect of GRPR-targeted TRT of prostate cancer increases when combined with mTOR inhibitor rapamycin.[28]

The clinical use of trastuzumab has been firmly established in the clinics over the past decades either as monotherapy or in combination with established cytostatic drugs or other targeted substances. The wide range of therapeutic combinations and good tolerability of trastuzumab should facilitate its implementation with TRT and external irradiation, not only in the treatment of prostate cancer but also for other cancers that are often treated with external beam therapy or TRT with the precondition that lesions express HER2. In a recent study, HER2 overexpression was detected in 2.7% of tissue samples collected from 37,992 patients suffering from different malignancies. HER2 overexpression was detected in bladder carcinomas (12.4%), gallbladder carcinomas (9.8%), extrahepatic cholangiocarcinomas (6.3%) or cervical carcinomas (3.9%).[39] Detection of HER2 could be confirmed either with IHC analysis of biopsy material or by molecular imaging using HER2-targeting probes. A recent clinical study demonstrated that even low HER2 expression could be detected using ^{68}Ga-ABY-025, the anti-HER2 affibody molecule used in our study.[40]

In conclusion, we have developed and characterized a promising GRPR-targeting radioligand ^{177}Lu-DOTAGA-PEG$_2$-RM26 and demonstrated its therapeutic efficacy *in vivo* in prostate cancer xenografts. Moreover, our study presents the first *in vivo* proof-of-principle that the effects of anti-GRPR radiotherapy can be amplified by coadministration of anti-HER2 treatment leading to prolonged survival.

References

1. Conde Moreno AJ, Ferrer Albiach C, Muelas Soria R, et al. Oligometastases in prostate cancer: restaging stage IV cancers and new radiotherapy options. *Radiat Oncol* 2014;9:258.
2. Chatalic KL, Kwekkeboom DJ, de Jong M. Radiopeptides for imaging and therapy: a radiant future. *J Nucl Med* 2015;56:1809–12.
3. Markwalder R, Reubi JC. Gastrin-releasing peptide receptors in the human prostate: relation to neoplastic transformation. *Cancer Res* 1999;59: 1152–9.
4. Ananias HJ, van den Heuvel MC, Helfrich W, et al. Expression of the gastrin-releasing peptide receptor, the prostate stem cell antigen and the prostate-specific membrane antigen in lymph node and bone metastases of prostate cancer. *Prostate* 2009;69:1101–8.
5. Bodei L, Paganelli G, Mariani G. Receptor radionuclide therapy of tumors: a road from basic research to clinical applications. *J Nucl Med* 2006;47:375–7.
6. Ginj M, Zhang H, Waser B, et al. Radiolabeled somatostatin receptor antagonists are preferable to agonists for in vivo peptide receptor targeting of tumors. *Proc Natl Acad Sci USA* 2006;103: 16436–41.
7. Cescato R, Maina T, Nock B, et al. Bombesin receptor antagonists may be preferable to agonists for tumor targeting. *J Nucl Med* 2008;49:318–26.
8. Llinares M, Devin C, Chaloin O, et al. Syntheses and biological activities of potent bombesin receptor antagonists. *J Pept Res* 1999;53:275–83.
9. Mansi R, Wang X, Forrer F, et al. Evaluation of a 1,4,7,10-tetraazacyclododecane-1,4,7,10-tetraacetic acid-conjugated bombesin-based radioantagonist for the labeling with single-photon emission computed tomography, positron emission tomography, and therapeutic radionuclides. *Clin Cancer Res* 2009;15:5240–9.
10. Tolmachev V, Orlova A. Influence of labelling methods on biodistribution and imaging properties of radiolabelled peptides for visualisation of molecular therapeutic targets. *Curr Med Chem* 2010;17:2636–55.
11. Varasteh Z, Rosenström U, Velikyan I, et al. The effect of mini-PEG-based spacer length on binding and pharmacokinetic properties of a 68Ga-labeled NOTA-conjugated antagonistic analog of bombesin. *Molecules* 2014;19:10455–72.
12. Varasteh Z, Mitran B, Rosenström U, et al. The effect of macrocyclic chelators on the targeting properties of the 68Ga-labeled gastrin releasing peptide receptor antagonist PEG2-RM26. *Nucl Med Biol* 2015;42:446–54.
13. Mitran B, Varasteh Z, Selvaraju RK, et al. Selection of optimal chelator improves the contrast of GRPR imaging using bombesin analogue RM26. *Int J Oncol* 2016;48:2124–34.
14. Garske-Román U, Sandström M, Fröss Baron K, et al. Prospective observational study of 177Lu-DOTA-octreotate therapy in 200 patients with advanced metastasized neuroendocrine tumours (NETs): feasibility and impact of a dosimetry-guided study protocol on outcome and toxicity. *Eur J Nucl Med Mol Imaging* 2018;45:970–88.
15. Wadosky KM, Koochekpour S. Molecular mechanisms underlying resistance to androgen deprivation therapy in prostate cancer. *Oncotarget* 2016; 7:64447–70.
16. Yagoda A, Petrylak D. Cytotoxic chemotherapy for advanced hormone-resistant prostate cancer. *Cancer* 1993;71:1098–109.
17. Reynolds AR, Kyprianou N. Growth factor signalling in prostatic growth: significance in tumour development and therapeutic targeting. *Br J Pharmacol* 2006;147(Suppl 2):S144–52.
18. Craft N, Shostak Y, Carey M, et al. A mechanism for hormone-independent prostate cancer through modulation of androgen receptor signaling by the HER-2/neu tyrosine kinase. *Nat Med* 1999;5:280–5.
19. Signoretti S, Montironi R, Manola J, et al. Her-2-neu expression and progression toward androgen independence in human prostate cancer. *J Natl Cancer Inst* 2000;92:1918–25.
20. Andersson J, Rosestedt M, Orlova A. Imaging of HER2 may improve the outcome of external irradiation therapy for prostate cancer patients. *Oncol Lett* 2015;9:950–4.
21. Lymperis E, Kaloudi A, Sallegger W, et al. Radiometal-dependent biological profile of the radiolabeled gastrin-releasing peptide receptor antagonist SB3 in cancer theranostics: metabolic and biodistribution patterns defined by neprilysin. *Bioconjug Chem* 2018;29:1774–84.

Cancer Therapy and Prevention

22. Ahlgren S, Orlova A, Wållberg H, et al. Targeting of HER2-expressing tumors using 111In-ABY-025, a second-generation affibody molecule with a fundamentally reengineered scaffold. *J Nucl Med* 2010;51:1131–8.

23. Larsson E, Strand SE, Ljungberg M, et al. Mouse S-factors based on Monte Carlo simulations in the anatomical realistic Moby phantom for internal dosimetry. *Cancer Biother Radiopharm* 2007;22:438–42.

24. Carlson DJ, Stewart RD, Li XA, et al. Comparison of in vitro and in vivo alpha/beta ratios for prostate cancer. *Phys Med Biol* 2004;49:4477–91.

25. Emmett L, Willowson K, Violet J, et al. Lutetium 177 PSMA radionuclide therapy for men with prostate cancer: a review of the current literature and discussion of practical aspects of therapy. *J Med Radiat Sci* 2017;64:52–60.

26. Wang H, Mu X, He H, et al. Cancer radio-sensitizers. *Trends Pharmacol Sci* 2018;39:24–48.

27. Kratochwil C, Bruchertseifer F, Rathke H, et al. Targeted α-therapy of metastatic castration-resistant prostate cancer with 225Ac-PSMA-617: dosimetry estimate and empiric dose finding. *J Nucl Med* 2017;58:1624–31.

28. Dumont RA, Tamma M, Braun F, et al. Targeted radiotherapy of prostate cancer with a gastrin-releasing peptide receptor antagonist is effective as monotherapy and in combination with rapamycin. *J Nucl Med* 2013;54:762–9.

29. Kim K, Zhang H, La Rosa S, et al. Bombesin antagonist-based radiotherapy of prostate cancer combined with WST-11 vascular targeted photodynamic therapy. *Clin Cancer Res* 2017;23:3343–51.

30. Mitran B, Thisgaard H, Rosenström U, et al. High contrast PET imaging of GRPR expression in prostate cancer using cobalt-labeled Bombesin antagonist RM26. *Contrast Media Mol Imaging* 2017;2017:6873684.

31. Nock BA, Maina T, Krenning EP, et al. "to serve and protect": enzyme inhibitors as radiopeptide escorts promote tumor targeting. *J Nucl Med* 2014;55:121–7.

32. Kaloudi A, Nock BA, Lymperis E, et al. Improving the in vivo profile of minigastrin radiotracers: a comparative study involving the neutral endopeptidase inhibitor phosphoramidon. *Cancer Biother Radiopharm* 2016;31:20–8.

33. Chatalic KL, Konijnenberg M, Nonnekens J, et al. In vivo stabilization of a gastrin-releasing peptide receptor antagonist enhances PET imaging and radionuclide therapy of prostate cancer in preclinical studies. *Theranostics* 2016;6:104–17.

34. Marsouvanidis PJ, Melis M, de Blois E, et al. In vivo enzyme inhibition improves the targeting of [177Lu]DOTA-GRP(13-27) in GRPR-positive tumors in mice. *Cancer Biother Radiopharm* 2014;29:359–67.

35. Fujimori K, Covell DG, Fletcher JE, et al. A modeling analysis of monoclonal antibody percolation through tumors: a binding-site barrier. *J Nucl Med* 1990;31:1191–8.

36. Malmberg J, Tolmachev V, Orlova A. Imaging agents for in vivo molecular profiling of disseminated prostate cancer: cellular processing of [(111)in]-labeled CHX-A″DTPA-trastuzumab and anti-HER2 ABY-025 affibody in prostate cancer cell lines. *Exp Ther Med* 2011;2:523–8.

37. Osman I, Mikhail M, Shuch B, et al. Serum levels of shed Her2/neu protein in men with prostate cancer correlate with disease progression. *J Urol* 2005;174:2174–7.

38. Maximiano S, Magalhães P, Guerreiro MP, et al. Trastuzumab in the treatment of breast cancer. *BioDrugs* 2016;30:75–86.

39. Yan M, Schwaederle M, Arguello D, et al. HER2 expression status in diverse cancers: review of results from 37,992 patients. *Cancer Metastasis Rev* 2015;34:157–64.

40. Sörensen J, Velikyan I, Sandberg D, et al. Measuring HER2-receptor expression in metastatic breast cancer using [68Ga]ABY-025 Affibody PET/CT. *Theranostics* 2016;6:262–71.

Cancer Therapy and Prevention